Looking at long molecules in solution: what happens when they are subjected to Couette flow?†

Alison Rodger,[a] Rachel Marrington,[a] Michael A. Geeves,[b] Matthew Hicks,[ac] Lahari de Alwis,[a] David J. Halsall[d] and Timothy R. Dafforn[c]

Received 3rd April 2006, Accepted 24th May 2006
First published as an Advance Article on the web 14th June 2006
DOI: 10.1039/b604810m

Knowing the structure of a molecule is one of the keys to deducing its function in a biological system. However, many biomacromolecules are not amenable to structural characterisation by the powerful techniques often used namely NMR and X-ray diffraction because they are too large, or too flexible or simply refuse to crystallize. Long molecules such as DNA and fibrous proteins are two such classes of molecule. In this article the extent to which flow linear dichroism (LD) can be used to characterise the structure and function of such molecules is reviewed. Consideration is given to the issues of fluid dynamics and light scattering by such large molecules. A range of applications of LD are reviewed including (i) fibrous proteins with particular attention being given to actin; (ii) a far from comprehensive discussion of the use of LD for DNA and DNA–ligand systems; (iii) LD for the kinetics of restriction digestion of circular supercoiled DNA; and (iv) carbon nanotubes to illustrate that LD can be used on any long molecules with accessible absorption transitions.

Introduction

Many molecules in biological systems are long (*e.g.* DNA) or part of long assemblies of molecules (*e.g.* fibrous proteins or membrane-bound molecules). While it is clear that the structures of such moieties are important to their function, many of the powerful techniques of structural biology, including X-ray diffraction and NMR spectroscopy, are not well suited to high order macromolecular complexes. Microscopies of various kinds are extremely useful but if working on molecular scales, almost by definition, focus on single units (molecules or arrays of molecules) at any one time rather than the whole population and the samples are also not fully in the solution phase. The purpose of this article is to illustrate the advantages and disadvantages of solution-phase flow linear dichroism (LD) spectroscopy for structural characterization of solutions of long molecules ranging from biomacromolecular systems to carbon nanotubes. Our recent work in this area has been inspired by the increased availability of samples for structural analysis which in turn has led us to develop a range of new Couette flow cells to reduce both sample volume and light scattering and to enable experiments under tight temperature control.[1–5] The way has now opened to many more applications that were previously impossible due to restricted sample quantity, required conditions or molecule size.

[a] *Department of Chemistry, University of Warwick, Coventry, UK CV4 7AL*
[b] *Department of Biosciences, University of Kent, Canterbury, UK CT2 7NJ*
[c] *Department of Biosciences, University of Birmingham, Birmingham, UK B15 2TT*
[d] *Department of Clinical Biochemistry, Addenbrooke's Hospital, Cambridge, UK CB2 2QR*

† The HTML version of this article has been enhanced with colour images.

Much of the flow linear dichroism literature relates to nucleic acids. The DNA work published before the early 1990s has been superbly reviewed by Nordén, Kubista and Kuruscev in ref. 6. An earlier linear dichroism review by Nordén is more general in subject matter.[7] The aim of this article is to cover the developments that have happened in the last ten years or so and to give an overview of how linear dichroism can be used to study a wide range of long molecules from DNA to fibrous proteins to carbon nanotubes. The intent here is to be illustrative rather than comprehensive, though the references cited open up a literature trail that should lead to most available literature.

Linear dichroism

Linear dichroism (LD) is a spectroscopic technique that can be used with systems that are either intrinsically oriented, or can be oriented during an experiment by external forces.[6–8] LD measures the difference in absorption of light linearly polarised parallel and perpendicular to an orientation axis,

$$LD = A_{\parallel} - A_{\perp}. \quad (1)$$

In the case of flow orientation of long molecules, the orientation axis is the long axis of the molecule. If a transition moment (the direction of net electron displacement during an electronic transition) is aligned more parallel than perpendicular to the orientation axis, a positive LD signal is observed. Conversely, if the direction of electron movement is more perpendicular than parallel to the orientation axis, a negative LD signal is observed. When a transition moment is at an angle of 54.7° the LD signal equals zero, however effective the orientation. Some transition polarizations of relevance for biomacromolecules are shown in Fig. 1.[2,9–11]

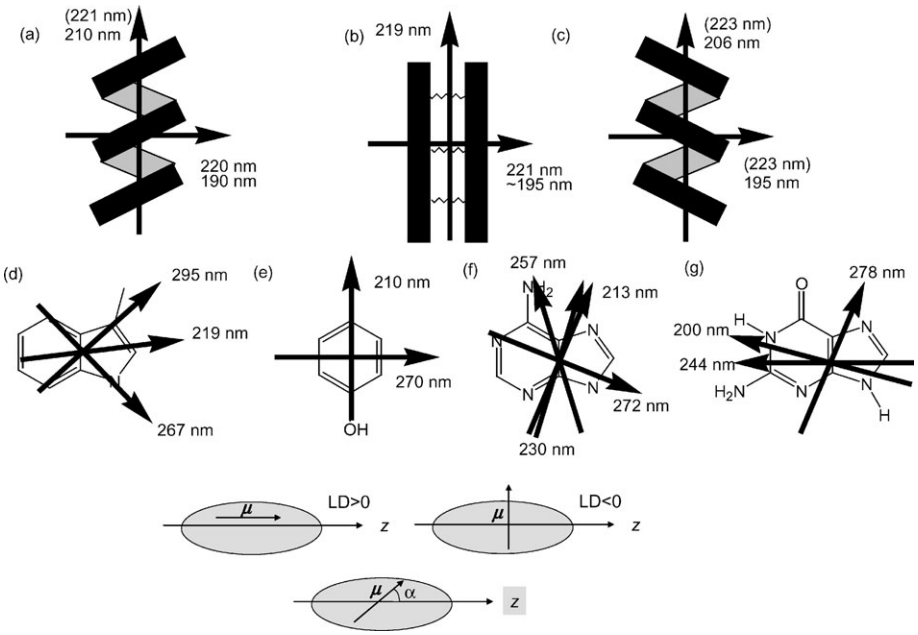

Fig. 1 The orientation of various polarization moments (a) α-helix (as determined by calculations[2]); (b) β-sheet (as determined by calculations[2]); (c) poly-proline type II helix (as determined by calculations[2]); (d) tryptophan;[9] (e) tyrosine; (f) adenine[10] and (g) guanine[11] chromophores together with LD schematic.

The reduced linear dichroism LD^r is often a convenient pathlength- and concentration-independent summary of LD data for quantitative analysis:

$$LD^r = \frac{LD}{A} = \frac{A_{||} - A_{\perp}}{A} = \frac{3}{2}S(3\cos^2\alpha - 1) \qquad (2)$$

where A is the absorption of the sample under isotropic conditions *i.e.* not oriented, and S a scaling factor (the orientation factor) defining the efficiency of the macroscopic orientation. For uniaxial rods, S equals 1 for perfect orientation, and 0 for random orientation. α (Fig. 1) is defined as the angle between the transition moment responsible for the absorption of light at a particular wavelength and the orientation axis. If either S or α is known the other can be calculated.

Molecules can be aligned using a number of techniques,[6–8,12] the most common being stretched film and flow orientation, which is the focus of this article. Flow orientation is ideal for biological molecules and others where the sample needs to be hydrated.[12–15] The orientation of long polymers is effected by the viscous drag created when a solution is flowed between narrow walls. A Couette flow LD cell, where a solution is placed in the annular gap between two cylindrical cells, one of which rotates and causes alignment of the molecules, has proved to be the most sample-efficient method of achieving this. A schematic diagram of a Couette cell is given in Fig. 2. For efficient alignment, the flow must be laminar, not turbulent.

Couette cells are derived from the work of Maurice Frédéric Alfred Couette and Henry Reginald Arnulph Mallock, who in the late 1800s independently developed a means to measure viscosity based on shearing a liquid between coaxial cylinders.[16–18,26] Since then there have been many applications of the Couette principle within the engineering and physics communities, the most notable example being Taylor–Couette flow which is a term used to define the flow between rotating cylinders.[27–29]

The modern incarnation of the Couette system developed in 1964 by Wada and Kozawa[20] involves one cylinder being inserted inside another and the solution flowing between the narrow gap (annular gap) as it is dragged by the rotation of one of the cylinders (Fig. 2). One of the cylinders must be transparent to the radiation being used and the other needs a transparent light path for the light which is incident radially on the cell (Fig. 2). The annular gap has typically been 500 μm, though experiments using a 50 μm annular gap have been reported.[13,15] In order to orient the sample it is necessary for the inner and outer cylinders to rotate at different speeds, therefore, creating a viscous drag and flow gradient in the solution; usually one cylinder is stationary. Previous studies have used either a rotating inner and fixed outer cylinder *e.g.* ref. 20 and 30, or a rotating outer and fixed inner cylinder *e.g.* ref. 31 and 32. The latter offers more flow stability but there are advantages for both options. In both cases it is necessary

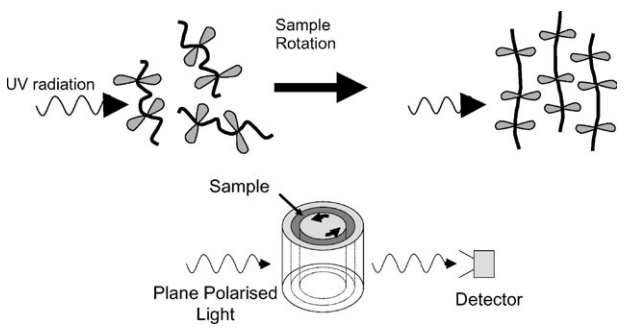

Fig. 2 Schematic diagram of a Couette flow cell.

that the light path through the cell allows optimal transmission, *i.e.* the rotating component and the region which is stationary where the light beam is incident need to be transparent to the radiation used. For example, for UV applications quartz is the most common material (though calcium fluoride has also been used[15]). The light beam can be either perpendicular[20] or parallel[31] to the axis of rotation. The perpendicular orientation is more common and is the one adopted in all studies detailed here.

Linear dichroism spectra are usually collected using a converted circular dichroism spectropolarimeter. The circularly polarised light of a CD spectropolarimeter is converted to linearly polarised light by the addition of a quarter wave plate, or as in our experiments, the photo elastic modulator 1/4 wave plate is converted to a 1/2 wave plate and the required alternating polarizations of light are produced directly by the instrument. Alternatively one can use polarisers in a normal absorption spectrometer and manually rotate the polarisers or the sample (though the latter is challenging for a Couette flow cell). The former option has significantly better signal to noise ratios. The linearly-polarised light passes through the sample and interacts with the oriented molecules to yield a net LD signal. As with all absorbance spectroscopy techniques a baseline must be subtracted from the sample spectrum. There are in principle two options for the baseline in a flow LD experiment. The first is to stop (or almost stop) the flow and measure the signal. With Couette flow cells this requires that either the rotating unit is optically uniform or that a very stable extremely low rotation speed is able to be maintained. The former is the case for our recently designed micro-volume Couette LD cells where the outer rotating cylinder is an extruded quartz capillary. Alternatively, one replaces the sample with buffer or solvent and rotates the unit as for the sample.

Fluid dynamics of flow in concentric cylinder flow cells

A fluid is a substance that will deform continuously when it is subjected to a tangential or shear force.[33] In the case of a Couette system, a velocity is imposed on the fluid contained between two concentric cylinders as one of these cylinders rotates (Fig. 2). The viscosity of a fluid (its resistance to shear or flow) will affect its dynamics. In all examples detailed in this work the solutions are aqueous so can be assumed to act predominantly like water, and therefore have constant viscosity independent of shear gradient, as discovered by Couette[26] (though high concentrations of sample increase the viscosity). Different flow states within the system exist, and it is these states that have been the subject of much study over the years since the work of Mallock and Couette.[16–19,26] The most notable work is that of Sir Geoffrey Ingram Taylor who investigated the flow stability of a viscous fluid when two cylinders rotate in the same direction and in opposite directions[27] and later went on to conclude that if only the outer cylinder rotates the flow is more stable than if only the inner cylinder rotates.[28] He also went on to study the effect of rotation speed and investigate the effect this has on fluid stability.

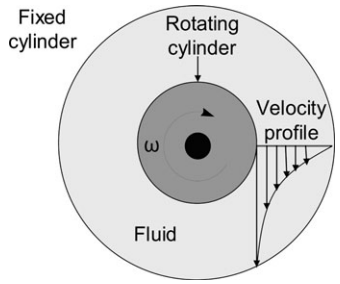

Fig. 3 Fluid flow profiles for inner rotating cylinder set-up, viewed from above. The longer the arrow describing the direction of the fluid flow, the faster the flow speed. Figure reproduced from R. Marrington, T. R. Dafforn, D. K. Halsall, M. Hicks and A. Rodger, *Analyst*, 2005, **130**, pp. 1608–1616—Reproduced by permission of the Royal Society of Chemistry.[4]

The spinning of either cylinder in a co-centric cylinder system, as in the LD cells of Fig. 2, causes the fluid in the annular gap to flow in a pattern dependent on many parameters in the system, including: the rotation speed of the cylinder, which cylinder rotates, the viscosity of the fluid, and the potential for interaction between the surface of the cylinder and the fluid or molecules in the fluid.[4,34] The flow profile for an inner rotating cylinder is given in Fig. 3.[33] Transitions between states are determined as functions of the inner and outer cylinder Reynolds numbers R_i and R_o, respectively. The Reynolds number is named after Osbourne Reynolds[35,36] and is a dimensionless variable that indicates the relative significance of the viscous effect compared to the inertia effect. The Reynolds number (Re) in the form applicable for a fluid in the annulus between two concentric cylinders is defined (kg s^{-1} m^{-1})

$$Re = \frac{\omega_1 r_1 \delta}{\nu} \tag{3}$$

where ω_1 is the angular velocity of one rotating cylinder in rad s^{-1}, r_1 is the radius of that rotating cylinder in m, δ is the gap width ($r_2 - r_1$) in m, and ν is the kinematic viscosity in m^2 s^{-1} (kinematic viscosity is equal to absolute or dynamic viscosity divided by density).[37] At high Re, the flow changes from laminar Couette flow to a series of more complex states, the first of which involves the appearance of Taylor vortices (vertically stacked toroids of flow around the inner cylinder) and the next involves wavy vortex flow which is exactly what the name says. These can be visualised by introducing light-reflecting suspended material into an LD cell as illustrated in Fig. 4. In practice we found that the Taylor vortices and wavy vortices could only be visualised in our original LD cell.[12] Our more recent and better engineered cells proved to have much more stable flow. Although Taylor vortex flow is still essentially horizontal as in Couette flow, the slow twisting rotation of the individual toroids is likely to have an effect on the alignment of molecules and it may depend on their flexibility. For example, we have observed that ethidium bromide bound to DNA is differently oriented in Couette flow and Taylor vortex flow regimes, presumably due to the different stiffness of the DNA with and without the intercalator ethidium bromide.[4]

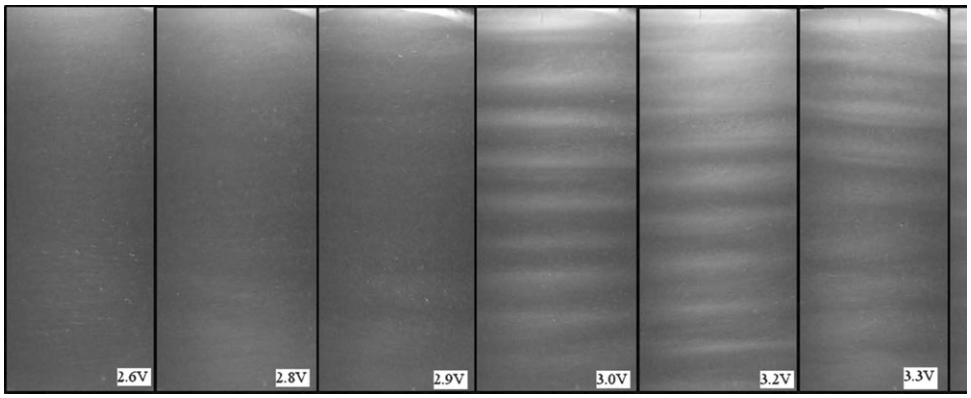

Fig. 4 Images of AQ-1000 rheoscopic fluid (titanium dioxide coated mica flakes in silicone oil, Kalliroscope gallery, 264 Main Street, P.O. Box 60, Groton, Massachusetts 01450, USA. http://www.kalliroscope.com) at a concentration of 5% in water in a concentric cylinder LD cell rotating at different speeds (speed increases linearly with voltage). A light source was shone onto the cell from above to illuminate the flakes. The AQ-1000 flakes align along the direction of fluid flow, providing an insight into the actual fluid flow in the cell. A 1 cm high slice through the middle of the cell window is illustrated at voltages from 2.6–3.5 V.

Light scattering correction

One of the challenges of working with high order macromolecular complexes, *e.g.* protein fibres or carbon nanotubes, is that they scatter light. The lenses of the microvolume capillary LD cells reduce this effect but it is still an issue, see *e.g.* ref. 38 and 39. The problem arises because the spectrometer simply measures the light that reaches the detector and assumes that which does not has been absorbed. Thus scattered photons are assumed to have been absorbed. A significant part of this problem can be removed by collecting the light as close to the LD cuvette as possible—this can be achieved by a number of methods including locating the photomultiplier tube (PMT) very close to the sample, increasing the angle of acceptance of the PMT, or locating a lens just after the sample to gather the light onto the PMT. However, even this does not always result in the desired flat line in the LD spectra outside absorbance regions. In such cases, the method of Nordh and others[39] can be used to subtract the scattering contribution to the signal as follows. Absorbance LD (LD^{A}) and background turbidity dichroism (LD^{τ}) contribute to the total LD signal as shown by eqn (5).

$$LD_{\text{total}} = LD^{A} + LD^{\tau}. \quad (5)$$

The wavelength dependence of LD^{τ} is accounted for by linear regression of eqn (5) to a function:

$$LD^{\tau}(\lambda) = a\lambda^{-k} \quad (6)$$

where k is a constant that has been shown generally to relate to the unpolarised turbidity (and usually takes values between 2.8 and 3.5), and a is a constant.[39] The implementation of this method is illustrated in Fig. 5.

Applications of linear dichroism

In the 1960s–1970s flow LD was recognised as a key technique and was used in the characterisation of fibrous proteins such as actin as well as for probing the orientation of DNA and bound ligands.[21–24] The limitations of instrument design and technology then, in particular the sample volume required (1–2 mL), and spectrometer design made it difficult to develop the technique further. The main applications reported in the literature lie in the analysis of nucleic acids,[25] mainly because of the research interests of groups with Couette flow cells and also because proteins can be difficult to orient (globular proteins), or generate artefacts due to light scattering caused by their large size. In the remainder of this article the applications of LD to a range of systems will be summarised. It should be noted that the discussion of DNA applications is far from complete due to space limitations.

Fibrous proteins

The cytoskeleton of a cell is a network of protein fibres whose repeat unit is a whole protein molecule and which form microtubules and microfilaments in the cytoplasm. The cytoskeleton is critical to cell motility (cell movement) and cell

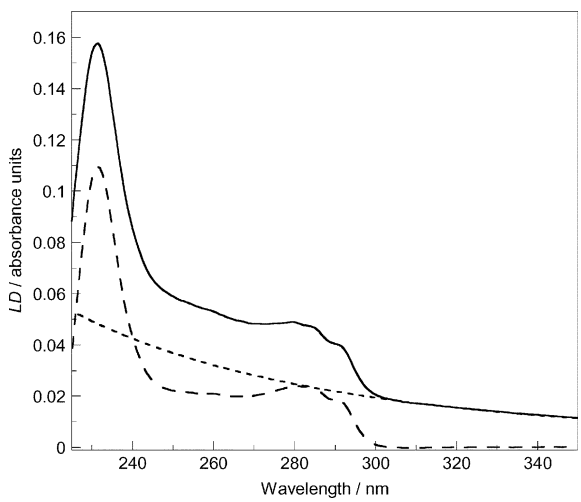

Fig. 5 A plot to show the method of light scattering correction when applied to a polymerised tubulin LD spectrum: the experimental data (—) (from which a baseline of the same sample in a non-rotating cell has been subtracted), the calculated turbidity LD, using a k value of 3.5, with a determined by rescaling the curve at 320 nm where there is no intrinsic absorbance (- - -), and the corrected data is (– – –).

morphology as well as processes such as cell division. It is not a rigid permanent structure, it is dynamic and constantly rearranges by polymerising and depolymerising to produce movement. There are three major types of protein fibre within the cytoskeleton of eukaryotic cells: actin filaments; intermediate filaments; and tubulin microtubules which are held together by protein–protein interactions. Apart from having structural roles within the cell, both tubulin microtubules and actin filaments also serve as 'tracks' for the biological movement of motor proteins—dyneins and kinesins along microtubules and myosins along actin filaments. More recently, interest has grown in fibrous proteins implicated in the mechanism of disease for such disorders as Alzheimer's and bovine spongiform encephalitis (prions). LD can be used to study these systems as discussed below. Actin was the first fibrous protein to be studied by Couette flow LD and recently we have improved the quality of data one can collect for such a system and also devised a range of new experiments. It is therefore an ideal case study to show possibilities of LD of fibrous proteins and is explored in some detail below. A brief review of work on other protein fibres is given after the discussion of actin.

Actin and actin-binding proteins. Actin exists as a globular monomer called G-actin which polymerises spontaneously to F-actin filaments in physiological conditions in the presence of ions such as Mg^{2+}, K^+ or Na^+. The process is reversible, in that when the ionic strength of the solution is lowered F-actin disassembles to G-actin monomers.[40] Actin binds 5′-adenosine triphosphate (ATP) or 5′-adenosine diphosphate (ADP)[41] which stabilise the fibre, but are not required for polymerisation. The three dimensional structure of actin molecules and actin filaments was solved in 1990 by Kenneth Holmes, Wolfgang Kabsch, and their colleagues.[42]

The polymerisation of actin has been a subject of interest for many years. The most common methods of analysis include viscometry, sedimentation, fluorescence spectroscopy, electron microscopy and light scattering, all of which have their merits. The initial application of Wada's Couette LD instrument in the 1960s and 1970s was to the study of F-actin solutions with a view to understanding the mechanism of muscle contraction.[21,24,43–45] Higashi and Oosawa, using the apparatus developed by Wada and Kozawa in 1964,[20] were able to investigate the orientation of aromatic amino acid residues (tyrosine and tryptophan) and bound adenine nucleotides. They reported that F-actin oriented by flow shows a negative dichroism at about 260 nm (due to adenine), a positive one at about 280 nm (tyrosine and tryptophan) and another negative one at about 295 nm (tryptophan).[21]

The use of LD to study actin did not proceed further at that time as it was concluded that the sensitivity of the apparatus needed to be improved to reduce light scattering and allow data collection at lower wavelengths.[45] Recent developments in spectrometer instrumentation and our new capillary Couette cells provide the required improvement and as shown below it is now possible to use LD as a technique either for, *e.g.*, the screening of actin–ligand binding or deciphering structural characteristics of the protein.[13]

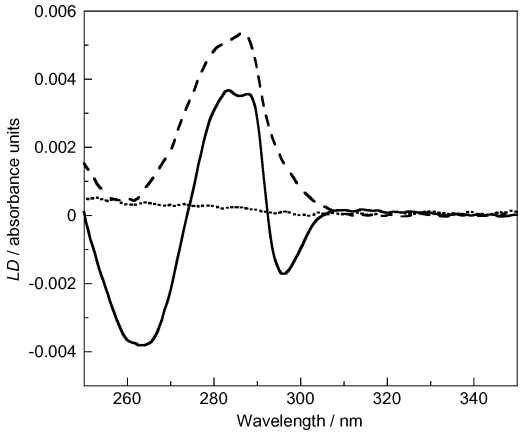

Fig. 6 Near UV LD spectra of actin (50 μM) (—); myosin S1 (50 μM) (- - -) and actin (50 μM)-myosin S1 (50 μM) (– – –) in KCl (15 mM); $MgCl_2$ (0.75 mM) and MOPS (3 mM) pH 7. The LD spectrum of unlabelled actin (50 μM)–myosin S1 (50 μM) has been corrected for baseline light scattering (k = 3.5, zeroing at 450 nm).

Fig. 6 shows a near UV LD spectrum of actin at 50 μM (see Appendix for experimental methods) which is consistent with those in the literature.[46] Far UV LD data for the backbone of actin was first collected using LD by Dafforn *et al.* in 2004.[13] The far UV LD spectrum of actin[46] at concentrations from 12–94 μM is shown in Fig. 7 and shows positive signals for both the n → π* transitions and the higher energy component of the π → π* transition, the lower energy component of the π → π* is evident as the 215 nm dip in the spectra. The LD therefore indicates that, on average, the α-helices in the fibre are oriented more perpendicular than parallel to the fibre axis in accord with literature data. Care must be taken in collecting low wavelength data for a system such as actin where light scattering is significant as illustrated in Fig. 7 where diluting the sample leads to an apparent wavelength shift of the maximum LD signal of ~30 nm to shorter wavelengths. When the dilution effect is simply to reduce the signal intensity according to the Beer Lambert law, then we can conclude the spectrum is real. From Fig. 8 it can be concluded that the LD wavelength maximum of the higher energy component of the π → π* transition is at 197.5 nm, in contrast to the previously reported maximum at 200 nm.[13] In all such experiments on fibrous proteins in general and actin in particular it is important to investigate the stability of the formed fibres to sheer forces by measuring the LD as a function of rotation speed.

The monomeric G-actin has no orientation in the flow, therefore the LD signal (shown in Fig. 7b at 222 nm) provides a convenient signal to follow the process of polymerization.[13] LD also provides a way to monitor the binding of globular proteins to fibrous proteins since globular molecules will not normally orientate in a flow cell, but upon binding to actin they do. The myosin motor domain (or subfragment 1, S1) binds tightly and stoichiometrically to F-actin. On its own, it has no LD spectrum (Fig. 6) but when bound to actin its near UV spectrum is distinct from the F-actin spectrum with loss of the negative peaks at 295 and 275 nm and enhanced 285 and 290 nm positive peaks reflecting the differences in the average

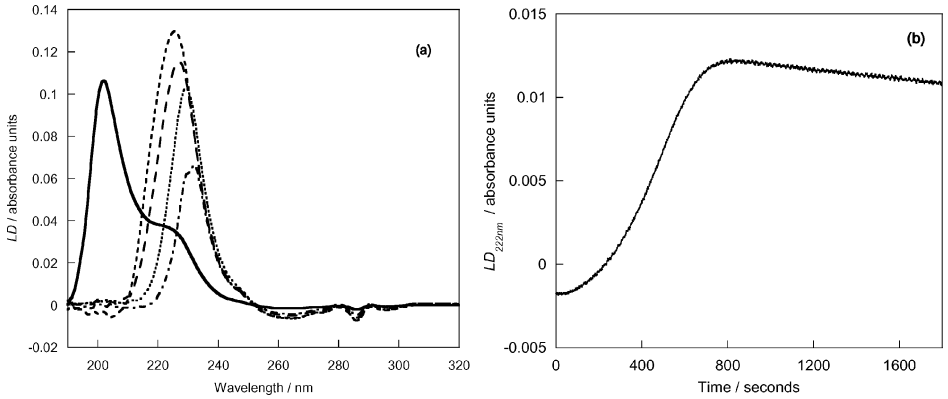

Fig. 7 (a) Far UV LD spectra showing the apparent shift to shorter wavelength of the maximum signal as the concentration of F-actin is reduced. F-actin concentrations 93; 74; 62; 53 and 12 μM (the true spectrum, solid line). (b) Polymerisation of G-actin into F-actin (~0.4 mg mL^{-1}) with ATP present (a) kinetics analysis monitoring LD_{222nm}.

orientations of aromatic residues in actin and the actin–myosin complex.

Tropomyosin is another actin-binding protein, but in this case it is itself a linear molecule and it binds to actin with a low stoichiometry of A_7Tm. Tropomyosin (Tm) is a coiled-coil protein that aligns in Couette flow and has its own LD spectrum, as first reported in ref. 47 where data were collected with a large-volume LD cell down to ~210 nm. The LD spectrum of Tm (Fig. 9) has a broad negative LD signal between 218–240 nm (n → π* transition) and a positive LD maxima at 206 nm.[46] Below 206 nm the LD signal tends negative. At higher concentrations a positive LD signal in the near UV at 280 nm due to the tyrosines (Tm contains no tryptophans) is apparent. Tm is a highly helical protein (>90% α-helices[48]), and the n → π* transition of the α-helices is perpendicular to the orientation axis, so its negative LD is consistent with the α-helices being more parallel than perpendicular to the orientation axis, as one would expect for a coiled-coil. The presence of Tm bound to actin has little effect on the LD spectrum of actin, largely because of the weak Tm signal. Tm forms a 1 : 1 complex with troponin (Tn, a globular protein which therefore has no intrinsic flow LD signal) which then binds to actin in a 7 : 1 : 1 ratio. Fig. 10 shows LD spectra of phalloidin-stabilised actin (psA, to make extended data collection feasible), Tm and Tn individually, psA-Tm and psA-Tn mixtures and in a 1 : 1 : 1 mixture to ensure saturation of actin with Tm and Tn. Tn increases the psA signal slightly, Tm shifts its maximum wavelength and also leads to a slightly increased signal, whereas the 1 : 1 : 1 mixture spectrum has both a shift of wavelength and a 30% larger LD signal. These data indicate that Tn's main effect is on the orientation factor of the fibre. Upon addition of $CaCl_2$, the LD spectrum (of psA–Tm–Tn–Ca^{2+}) overlays that of psA–Tm consistent with calcium causing the Tn–actin interaction to weaken (data not shown). Near UV LD studies by Yanagida *et al.* in 1974 on the effect of Ca^{2+} on the F-actin–Tm–Tn complex showed about a 20% decrease in intensity of the two negative peaks at 260 and 295 nm, and concluded that the presence of calcium made the fibre more flexible.[24,45] Taniguchi reported an even larger decrease in LD intensity upon the addition of calcium ions.

Near UV LD of actin (21 μM) and its complex with Tm (3 μM), Tm–Tn (3 μM) and Tm–Tn–Ca^{2+} (Tm–Tn 3 μM and Ca^{2+} 3 mM) are shown in Fig. 11.[46] It can be seen that there is an increase in signal intensity of the 285 nm transition (tyrosine and tryptophan) upon binding of Tm, and even

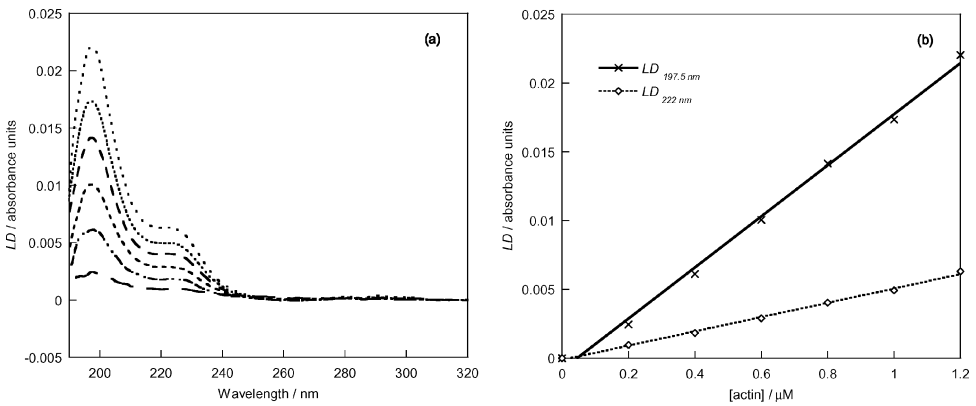

Fig. 8 The concentration dependence of the LD of solutions of F-actin at low concentrations, (a) wavelength LD spectra with F-actin concentrations of 1.2 (···); 1.0 (·····); 0.8 (– – –); 0.6 (- - - -); 0.4 (· ·– –) and 0.2 μM (—·), and (b) linear plots showing that the Beer Lambert law is obeyed at the concentrations shown.

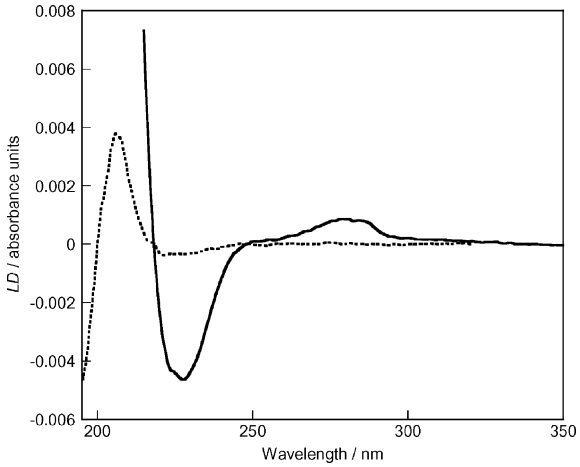

Fig. 9 LD spectra of tropomyosin at 50 (——) and 10 μM (- - - -) in KCl (20 mM), $MgCl_2$ (1 mM) and MOPS (4 mM) pH 7.

more so (by ~30%) upon binding of the Tm–Tn complex. The ADP region (265 nm) shows a slight increase upon addition of Tm to actin, with no noticeable change recorded for the addition of Tm–Tn to actin. There is no obvious difference in the tryptophan signal at 295 nm except for the binding of the Tm–Tn complex to actin. The effect of the addition of calcium to the system reduced all three signals by ~30%. This is consistent with literature data, though no change in the 285 nm transition had previously been reported. This may be due to the methods employed for the correction of scattering when these analyses were originally undertaken. As concentrations of greater than 100 μM were used in 1970s, light scattering artefacts were very significant in the spectra collected.

When using linear dichroism to detect the binding between a fibrous protein and globular protein (such as actin and myosin) it can be difficult to determine whether changes in the LD are due to the globular protein once it is oriented and/or whether there is a change in the orientation of the fibre as a whole or even its subunits. To aid in the interpretation of such

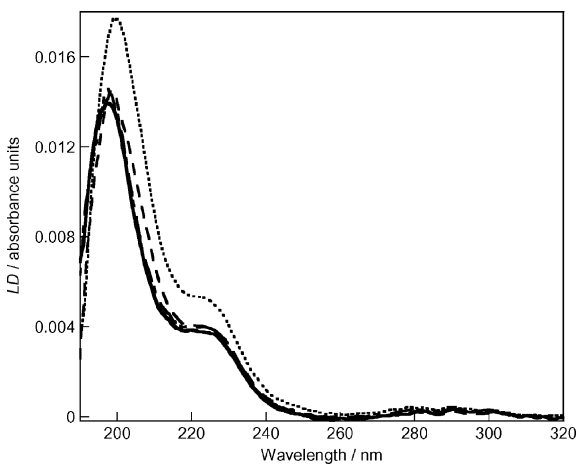

Fig. 10 (a) LD of phalloidin stabilised actin (psA) (——), psA–Tn (– – –); psA–Tm (- - - -); psA–Tm–Tn (. . ...). All protein concentrations are 1 μM. All solutions contain KCl (15 mM); $MgCl_2$ (0.75 mM) and MOPS (3 mM) pH 7.

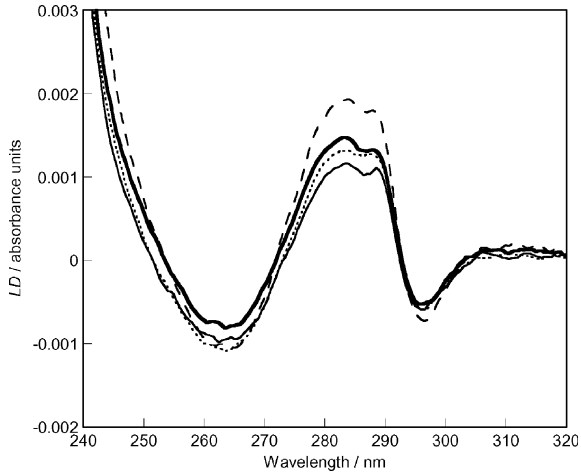

Fig. 11 Near UV LD spectra of actin (A) (21 μM) (——); A (21 μM)–tropomyosin (Tm) (3 μM) (. . . . .); A (21 μM)–Tm (3 μM)–Troponin (Tn) (3 μM) (- - - -) and A (21 μM)–Tm (3 μM)–Tn (3 μM)–Ca^{2+} (3 mM) (——). All solutions contained KCl (15 mM); $MgCl_2$ (0.75 mM) and MOPS (3 mM) pH 7.

spectra a probe molecule attached to the fibre that allows the orientation factor to be evaluated is required. The ideal probe has yet to be found, but Fig. 12 shows that probes can be readily detected. Rhodamine labelled phalloidin is attractive as the phalloidin stabilises the actin filaments without affecting the structure (rhodamine-labelled phalloidin stabilised actin and actin have very similar shaped LD spectra in the UV despite contributions from the ligand) and rhodamine has a large extinction coefficient (106 000 M^{-1} cm^{-1} at 542.75 nm[49]) and the signals are linear with concentration.

Far UV LD of other fibrous proteins

As noted above, actin was the first protein fibre to which Couette flow *LD* was applied in the near UV wavelength region and it is now possible to collect far UV data on such a system. A similar story can be told for tubulin (where α,β-tubulin heterodimers nucleate into oligomers, which then form protofilaments, with the subunits aligned head to tail with dimeric units repeating every 8 nm). Early experiments probed the near UV[38] or used the turbidity LD signal outside the absorbance region to follow polymerisation.[39] Backbone data for tubulin have more recently been collected and used to monitor chromophore reorientation during the polymerisation process.[5] One of the challenges of tubulin is the need to hold the sample at 37 °C during polymerisation. Analysis of tubulin kinetics and binding of various ligands including Taxol™, colchicine, vincristine and DAPI have been probed in a microvolume Couette cell.[5]

Essentially any fibrous protein which stays in solution can be flow oriented; at least preliminary near and far UV LD data have been collected for prions,[50] Alzheimer's fibres, collagen, and α_1-antitrypsin.[11] LD has also been used to probe the processes involved in the polymerisation and bundling of the bacterial homologue of tubulin, FtsZ.[51] The *E. coli* FtsZ has no tryptophans so the near UV region of the spectrum can be

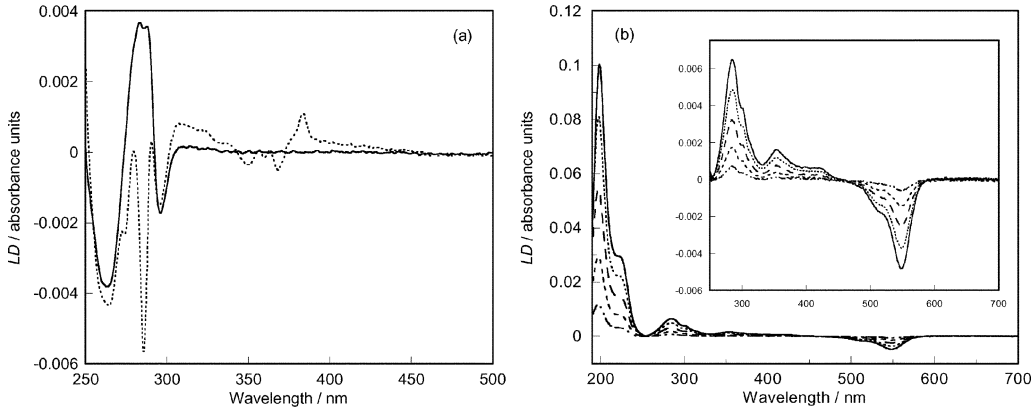

Fig. 12 (a) LD of actin (50 μM) (——) and pyrene labelled actin (50 μM) (· · · ·). (b) LD of rhodamine phalloidin labelled actin 10 (——), 8 (· · · ·), 6 (– – –), 4 (- - -) and 2 μM (· · – –) showing linear increase of LD signal with concentration.

interpreted in terms of contributions from guanine and tyrosines. This has been used to follow some of the structural changes which occur when the protofilaments bundle to form fibres. LD can also be used to probe the binding of another protein to a fibre. For example, the *E. coli* ortholog of the accessory protein Zap A, YgfE (which has been shown to be a bonafide division protein[52]) has been shown to promote FtsZ bundling at physiological concentrations.[52] During the bundling process LD shows that the guanine in GTP (which is sandwiched between successive FtsZ units) changes orientation. This has led to the proposal that macrochelation by a divalent metal cation to the terminal phosphate of GTP and the N7 nitrogen of guanine causes the conformational change of the guanine. However, whether this initiates or results from FtsZ polymer bundling is at present unknown.

DNA and DNA–ligand systems

An article with the chosen title would not be complete without at least some mention of DNA and DNA–ligand systems, due to the extensive literature available in this area. However, this also presents a problem as it is very difficult to give a representative view of the whole field. B-DNA is a long molecule whose base π–π* transitions all lie perpendicular to the helix axis in an idealised structure—thus giving rise to a negative signal under the DNA absorbance bands with a maximum magnitude at the same wavelength (almost) as the normal absorbance maximum. The consensus is that rather than 90°, a value of 86° should be used (though the 'true' value is probably less than this and depends on the flexibility (so environment and sequence) of a given piece of DNA). Chou and Johnson[53] extensively analysed the LD of DNA down to 175 nm in terms of the base transitions and found the average inclination of the bases is of the order of 20° from the helix axis.

One of the main applications of LD uses its ability to probe interactions between an oriented molecule and a species that can not be aligned by itself but aligns upon binding to the long molecule. Information regarding the corresponding binding geometries can be ascertained if transition moment directions of the components are known, or conversely. Molecules (usually cationic species) can bind to DNA by intercalation, groove binding or externally binding. Examples include dyes, metal complexes and proteins. There are a number of superb reviews on this area, as noted above.[6,7] The work of Schellman and collaborators and Nordén and collaborators has been particularly valuable. Table 1 gives examples of DNA–ligand complexes studied by LD.

When ligands are added to a solution of DNA and they bind, one expects to see signals due to the ligand transitions as well as the DNA. Ideally the ligand has no absorbance in the DNA region, so one can determine the DNA orientation parameter in the presence of the ligand. Intercalators are planar aromatic molecules and bind parallel to the DNA bases, so to a first approximation are expected to have LD^r values the same as the DNA bases. In practise, they locally stiffen the DNA so they and the bases near them are better oriented than other bases and the LD^r is greater in the ligand region.[8] Thus, if all ligand transitions have negative LD signals with LD^r values greater (due to increase in S) or equal in magnitude to those of the DNA bases, then one can be fairly sure that the ligand is intercalating. Alternatively, if long-axis polarised ligand transitions have positive LD signals, then a groove-binding mode is indicated. If there is a preference for AT-rich regions of DNA (where the groove is less sterically hindered) this supports this binding mode assignment.[54] If S is known, one can be more quantitative above this conclusion. If

Table 1 Examples of DNA–ligand complexes studied by LD. This table together with ref. 6 and 7 gives the beginning of a literature trail to find most systems which have been studied

Type of compound bound to DNA	Ligand bound to DNA	Ref.
Dyes	Ethidium Bromide	58
	DAPI	59
	Hoechst	60
	9-Hydroxyellipticine	61
Metal complexes	General	62
	Ruthenium metal complexes	63
		64
	Di-iron metal complexes	56
	Cobalt ammines	65
Proteins	Chromatin	66
	Rec-A	67

the only available ligand transition is in the DNA region one either has to hope S has not changed or hope that there is a wavelength where DNA can be probed independently of the ligand, as was the case for anthracene deriviatised with cationic spermine.[55] In this case a slight bending or stiffening of the DNA was observed. In the case of a tetracationic major groove binding di-iron helicate, the DNA was significantly bent locally to the ligand binding site, so the ligand orientation on the DNA cannot be determined. However, at low loading the bending per ligand was calculated.[56] An additional challenge in quantifying ligand orientation is that only bound ligands contribute to the LD signal but unbound ones contribute to the absorbance, thus making LD^{r} determinations challenging if the binding constant and the different extinction coefficients of free and bound ligand are not known.[57]

The extent of orientation of a DNA molecule depends on its flexibility and also its length. Simonson and Kubista[68] empirically related LD intensity to DNA length on the basis of the LD^{r} of some long DNAs of well-defined length:

$$LD^{r} = \frac{LD}{A} = -\frac{k_1 G}{k_2 + G} \qquad (7)$$

where A is the absorbance, G is the velocity gradient of the flow cell, $k_1 = 0.42$ for our experiment (from Fig. 8 of ref. 68), and the inverse of $1/k_2$ is proportional to the DNA length.

This equation has since been used to quantify the bending induced in DNA upon addition of a ligand.[56] The minimum length of DNA required to give an LD signal depends on the DNA flexibility and the desired signal : noise ratio. For easy data collection, 1000 or more base pairs are desirable. Less than 250 base pairs will be hard work—not surprisingly given that the persistence length (the length of DNA for it to bend though 1 rad) of DNA is typically $\sim$150 base pairs. Less quantitatively, changes in LD can be used to monitor single nucleotide polymorphisms since DNA mis-matches have an effect on DNA shape (hence scattering) and DNA orientation.[69]

Using molecular length to follow kinetics

LD is the ideal method to probe the kinetics of formation of protein fibres from assemblies of monomeric units as discussed above. It is also the ideal technique to follow such reactions as the effect of a restriction enzyme (DNA-cutting enzyme) as a function of time.[70] As illustrated in Fig. 13 if one begins with comparatively compact supercoiled circular DNA and adds a restriction enzyme the LD signal increases as the average length and hence orientation of the DNA increases. If the enzyme has two cut sites, then a subsequent decrease in LD is noticed as the average length decreases again. Perhaps the most intriguing thing about this experiment is that a supercoiled plasmid DNA (in this case $\sim$7000 base pairs in length) can be readily oriented—the starting point is not a zero LD signal. It is conceivable that, coupled with appropriate modelling, LD may be able to give information about the structures adopted by such a molecule.

LD is also ideal for following the progress of polymerase chain reactions (PCRs) or even simply monitoring the end point of a reaction.[71] In the latter case it can be used to determine viral load and by careful choice of primers this can be selective. The advantage of LD over other real time PCR methods is that primer-dimers, which plague most quantitative PCR methods, are invisible. Also, no additional labelling is required.

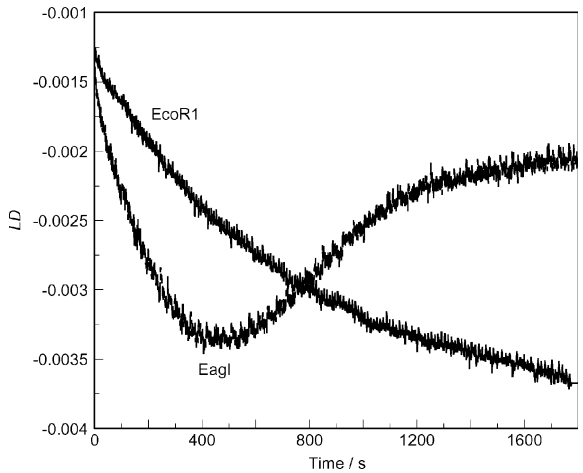

Fig. 13 Kinetics of restriction digests of a circular, super-coiled plasmid with *Eco*RI (which has a single cut site in the DNA sequence and thus single step kinetics) and *Eag*I (which has two cut sites in the DNA sequence).

Carbon nanotubes

Carbon nanotubes provide a final example for this article and 'proof' that one can use flow LD for any long molecule which can be put into solution and is spectroscopically active. Single walled carbon nanotubes (SWNTs) are soluble (more or less) in aqueous SDS. Despite the size of the SWNTs the scattering does not dominate the LD signal and the nanotube itself has a broad band in the far UV region of the spectrum.[72,73] Any small molecule which binds to DNA also acquires an LD signal, though in the case of aromatic molecules it is clear that there is significant coupling between the graphene sheets of the nanotubes and the π-systems of the ligand as well as inter-ligand interaction (as shown by the concentration dependence of the shape of the spectrum in Fig. 14).[70] Despite the negative charge of DNA we have also oriented DNA and the neutral PNA on SWNTs. The signs and magnitudes of the DNA signals should enable an accurate average orientation of the DNA on the SWNT to be determined if we know the orientation parameter. So far only qualitative analyses have been possible which indicate that DNA wraps around the nanotube in the opposite manner from PNA.[73]

Conclusion

Other recent applications of LD include the analysis of proteins and peptides in lipid bilayers, for example cytochrome *c* inserted into soybean liposome,[15] and the orientation of peptide fibres that are designed for molecular self assembly.[74] LD has also successfully been used to provide experimental evidence for models postulated by computer

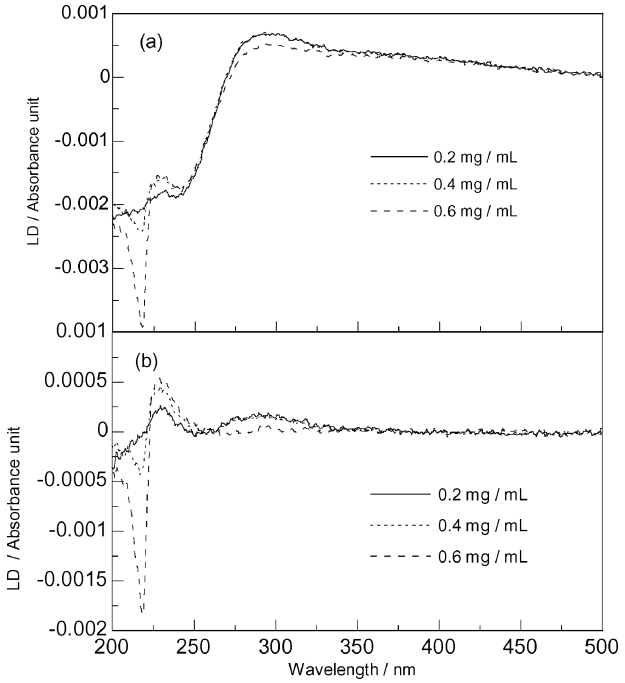

Fig. 14 (a) LD spectra of different concentrations of naphthalene in SWNTs (0.1 mg mL^{-1}) in SDS (9 mM) solution. SWNTs–naphthalene complexes were prepared by adding different amounts (0.2, 0.4 and 0.6 mg) of methanol dissolved naphthalene to 1 mL of SWNTs (0.1 mg mL^{-1}) in SDS (9 mM) solution and making final naphthalene concentrations of 0.2, 0.4 and 0.6 mg mL^{-1}. (b) Difference spectra obtained by subtracting the LD spectrum of SWNT (0.1 mg mL^{-1}) from the LD spectra of 0.2, 0.4 and 0.6 mg mL^{-1} naphthalene–SWNTs complexes.

simulations.[64] An ongoing project is the use of computer modelling programs for further structural characterisation of LD spectra of protein fibres.[15] So in conclusion it really does seem as if flow linear dichroism can be used to study any long molecule whose absorption spectrum is accessible.

Appendix: Materials and methods for actin studies

Unlabelled and pyrene-labelled actin were prepared using the methods detailed in ref. 75 and 76. Phalloidin-stabilised F-actin was prepared by incubating a solution of 10 μM actin (unlabelled or labelled) with 10 μM phalloidin for at least one hour at 4 °C.[77] Rhodamine phalloidin (R-415) was purchased from Molecular Probes. Using the information provided on the data sheet, a concentration of ~200 μM was prepared by dissolving the contents of the vial in 49.5 μL methanol (spectroscopic grade). Rhodamine-labelled phalloidin-stabilised actin was prepared by mixing rhodamine-labelled phalloidin and unlabelled actin in a 1 : 1 ratio at 10 μM for at least one hour at 4 °C. Tropomyosin (Tm) and troponin (Tn) were purchased from Sigma as lyophilized powder and solutions were prepared on the day of analysis. A relative molecular mass of ~65 kDa was assumed for Tm (calculated using Swiss-Prot accession numbers P04268 and P19352 for the α and β chains of tropomyosin from chicken[78]) with a purity of 99% (as stated on the container). A relative molecular mass of ~73.0 kDa was assumed for Tn (using Swiss-Prot accession numbers P02644; P12620 and P09860 for each subunit of Tn[78]), with a purity of 91% (as stated on container).

References

1 R. Marrington, T. R. Dafforn, D. J. Halsall and A. Rodger, *Biophys. J.*, 2004, **87**, 2002–2012.
2 A. Rodger, J. Rajendra, R. Marrington, M. Ardhammar, B. Nordén, J. D. Hirst, A. T. B. Gilbert, T. R. Dafforn, D. J. Halsall, C. A. Woolhead, C. Robinson, T. J. Pinheiro, J. Kazlauskaite, M. Seymour, N. Perez and M. J. Hannon, *Phys. Chem. Chem. Phys.*, 2002, **4**, 4051–4057.
3 A. Rodger, J. Rajendra, R. Marrington, R. Mortimer, T. Andrews, J. B. Hirst, A. T. B. Gilbert, D. Halsall, T. Dafforn, M. Ardhammar, B. Nordén, C. A. Woolhead, C. Robinson, T. Pinheiro, K. J. M. Seymour, N. Perez and M. J. Hannon, in *Biophysical Chemistry: Membranes and Proteins*, ed. R. H. Templer and R. Leatherbarrow, The Royal Society of Chemistry, Cambridge, 2002, pp. 3–19.
4 R. Marrington, T. R. Dafforn, D. J. Halsall, M. Hicks and A. Rodger, *Analyst*, 2005, **130**, 1608–1616.
5 R. Marrington, M. Seymour and A. Rodger, *Chirality*, 2006.
6 B. Nordén, M. Kubista and T. Kuruscev, *Q. Rev. Biophys.*, 1992, **25**, 51–170.
7 B. Nordén, *Appl. Spectrosc. Rev.*, 1978, **14**, 157–248.
8 A. Rodger and B. Nordén, *Circular Dichroism and Linear Dichroism*, Oxford University Press, Oxford, 1997.
9 B. Albinsson and B. Nordén, *J. Phys. Chem.*, 1992, **96**, 6204–6212.
10 A. Holmen, A. Broo, B. Albinsson and B. Norden, *J. Am. Chem. Soc.*, 1997, **119**, 12240–12250.
11 T. R. Dafforn, J. Rajendra, D. J. Halsall, L. C. Serpell and A. Rodger, *Biophys. J.*, 2004, **86**, 404–410.
12 A. Rodger, in *Methods in Enzymology*, ed. J. F. Riordan and B. L. Vallee, Academic Press, San Diego, 1993, vol. 226, pp. 232–258.
13 T. R. Dafforn, J. Rajendra, D. J. Halsall, L. C. Serpell and A. Rodger, *Biophys. J.*, 2004, **86**, 404–410.
14 L. B. A. Johansson and A. Davidsson, *J. Chem. Soc., Faraday Trans. 1*, 1985, **81**, 1375–1388.
15 A. Rodger, J. Rajendra, R. Marrington, M. Ardhammar, B. Norden, J. D. Hirst, A. T. B. Gilbert, T. R. Dafforn, D. J. Halsall, C. A. Woolhead, C. Robinson, T. J. T. Pinheiro, J. Kazlauskaite, M. Seymour, N. Perez and M. J. Hannon, *Phys. Chem. Chem. Phys.*, 2002, **4**, 4051–4057.
16 M. Couette, *Ann. Chim. Phys*, 1890, **6**, 433–510.
17 A. Mallock, *Proc. R. Soc. London*, 1888, **45**, 126.
18 A. Mallock, *Philos. Trans. R. Soc. London, Ser. A*, 1896, **187**, 41.
19 M. Kasai and F. Oosawa, *Methods Enzymol.*, 1972, **25**, 289–323.
20 A. Wada and S. Kozawa, *J. Polym. Sci., Part A*, 1964, **2**, 853–864.
21 S. Higashi, M. Kasai, F. Oosawa and A. Wada, *J. Mol. Biol.*, 1963, **7**, 421–430.
22 J. Hofricheter and W. Eaton, *Annu. Rev. Biophys. Bioeng.*, 1976, **5**, 511–560.
23 B. Nordén, *Appl. Spectrosc. Rev.*, 1978, **14**, 157–248.
24 F. Oosawa, Y. Maeda, S. Fujime, S. Ishiwata, T. Yanagida and M. Taniguchi, *J. Mechanochem. Cell Motil.*, 1977, **4**, 63–78.
25 B. Nordén, M. Kubista and T. Kurucsev, *Q. Rev. Biophys.*, 1992, **25**, 51–170.
26 R. J. Donnelly, *Phys. Today*, 1991, **November**, 32–39.
27 G. I. Taylor, *Proc. R. Soc. London, Ser. A*, 1923, **223**, 289–343.
28 G. I. Taylor, *Proc. R. Soc. London, Ser. A*, 1936, **157**, 546–564.
29 G. I. Taylor, *Proc. R. Soc. London, Ser. A*, 1936, **157**, 565–578.
30 A. Wada, *Biopolymers*, 1964, **2**, 361–380.
31 C. Lee and N. Davidson, *Biopolymers*, 1968, **6**, 531–550.
32 P. Oriel and J. Schellman, *Biopolymers*, 1966, **4**, 469–494.
33 J. O. Wilkes, *Fluid Mechanics for Chemical Engineers*, Prentice Hall PTR, Upper Saddle River, 1999.
34 C. D. Anderick, S. S. Liu and H. L. Swinney, *J. Fluid Mech.*, 1986, **164**, 155–183.
35 O. Reynolds, *Philos. Trans. R. Soc. London*, 1883, **174**, 935–982.
36 O. Reynolds, *Proc. R. Soc. London*, 1883, **35**, 84–99.
37 M. C. Potter and D. C. Wiggert, *Mechanics of Fluids*, Brooks/Cole Thomson Learning, Pacific Grove, 3rd edn, 2002.

38 M. Taniguchi and R. Kuriyama, *Biochim. Biophys. Acta*, 1978, **533**, 538–541.
39 J. Nordh, J. Deinum and B. Norden, *Eur. Biophys. J.*, 1986, **14**, 113–122.
40 E. D. Korn, M. F. Carlier and D. Pantaloni, *Science*, 1987, **238**.
41 S. L. Brenner and E. D. Korn, *J. Biol. Chem.*, 1984, **259**, 1441–1446.
42 K. C. Holmes, D. Popp, W. Gebhard and W. Kabsch, *Nature*, 1990, **347**, 44–49.
43 M. Miki and K. Mihashi, *Biophys. Chem.*, 1977, **6**, 101–106.
44 M. Taniguchi, *Electro–Opt. Dielectr. Macromol. Colloids*, 1979, 203–210.
45 T. Yanagida, M. Taniguchi and F. Oosawa, *J. Mol. Biol.*, 1974, **90**, 509–522.
46 R. Marrington, PhD Thesis, University of Warwick (Coventry), 2004.
47 M. J. Pandya, G. M. Spooner, M. Sunde, J. R. Thorpe, A. Rodger and D. N. Woolfson, *Biochemistry*, 2000, **39**, 8728–8734.
48 F. G. Whitby and G. N. Phillips, Jr, *Proteins: Struct., Funct., Genet.*, 2000, **38**, 49–59.
49 Molecular Probes, UK, 1993.
50 L. C. Serpel, 2003, unpublished data.
51 R. Marrington, E. Small, A. Rodger, T. R. Dafforn and S. Addinall, *J. Biol. Chem.*, 2004, **47**, 48821–48829.
52 F. J. Gueiros-Filho and R. Losick, *Genes Dev.*, 2002, **16**, 2544–2556.
53 P.-J. Chou and W. C. J. Johnson, *J. Am. Chem. Soc.*, 1993, **115**, 1205–1214.
54 B. Nordèn, S. Eriksson, S. K. Kim, M. Kubista, R. Lyng and B. Akerman, in *The Jerusalem Symposia on Quantum Chemistry and Biochemistry*, ed. B. Pullman and J. Jornter, Kluwer Academic Publishers, Dordrecht, 1990, vol. 23, pp. 23–41.
55 A. Rodger, I. S. Blagbrough, G. Adlam and M. L. Carpenter, *Biopolymers*, 1994, **34**, 1583–1593.
56 M. J. Hannon, V. Moreno, M. J. Prieto, E. Molderheim, E. Sletten, I. Meistermann, C. J. Isaac, K. J. Sanders and A. Rodger, *Angew. Chem., Int. Ed.*, 2001, **40**, 879–884.
57 D. Z. Coggan, I. S. Haworth, P. J. Bates, A. Robinson and A. Rodger, *Inorg. Chem.*, 1999, **38**, 4486–4497.
58 C. Houssier, B. Hardy and E. Fredercq, *Biopolymers*, 1974, **13**, 1141–1160.
59 M. Kubista, B. Akerman and B. Norden, *Biochemistry*, 1987, **26**, 4545–4553.
60 J. H. Moon, S. K. Kim, U. Sehlstedt, A. Rodger and B. Norden, *Biopolymers*, 1996, **38**, 593–606.
61 M. A. Ismail, K. Sanders, G. C. Fennell, H. C. Latham, P. Wormell and A. Rodger, *Biopolymers*, 1998, **46**, 127–143.
62 B. Nordén and F. Tjerneld, *FEBS Lett.*, 1976, **67**, 368–370.
63 K. K. Patel, E. A. Plummer, M. Darwish, A. Rodger and M. J. Hannon, *J. Inorg. Biochem.*, 2002, **91**, 220–229.
64 D. Z. M. Coggan, I. S. Haworth, P. J. Bates, A. Robinson and A. Rodger, *Inorg. Chem.*, 1999, **38**, 4486–4497.
65 A. Rodger, A. Parkinson and S. Best, *Eur. J. Inorg. Chem.*, 2001, **9**, 2311–2316.
66 F. Tjerneld, B. Nordén and H. Wallin, *Biopolymers*, 1982, **21**, 343–358.
67 B. Nordén, K. Mortensen, C. Elvingson, M. Kubista, B. Sjöberg, M. Ryberg and M. Takahashi, *J. Mol. Biol.*, 1991, **226**, 1175–1191.
68 T. Simonson and M. Kubista, *Biopolymers*, 1993, **33**, 1225–1235.
69 T. R. Dafforn, D. J. Halsall and A. Rodger, *Chem. Commun.*, 2001, 2410–2411.
70 M. R. Hicks, A. Rodger, C. M. Thomas, S. Blatt and T. R. Dafforn, *Biochemistry*, 2006, submitted for publication.
71 D. J. Halsall, T. R. Dafforn, R. Marrington, E. Halligan and A. Rodger, *IVD Technol.*, 2004, **6**, 51–60.
72 J. Rajendra, M. Baxendale, L. G. Dit Rap and A. Rodger, *J. Am. Chem. Soc.*, 2004, **126**, 11182–11188.
73 J. Rajendra and A. Rodger, *Chem.–Eur. J.*, 2005, **11**, 4841–4848.
74 M. J. Pandya, G. M. Spooner, M. Sunde, J. R. Thorpe, A. Rodger and D. N. Woolfson, *Biochemistry*, 2000, **39**, 8728–8734.
75 S. S. Lehrer and G. Kerwar, *Biochemistry*, 1972, **11**, 1211–1217.
76 A. H. Criddle, M. A. Geeves and T. E. Jeffries, *Biochem. J.*, 1985, **232**, 343–349.
77 R. Maytum, S. S. Lehrer and M. A. Geeves, *Biochemistry*, 1999, **38**, 1102–1110.
78 E. Gasteiger, A. Gattiker, C. Hoogland, I. Ivanyi, R. D. Appel and A. Bairoch, *Nucleic Acids Res.*, 2003, **31**, 3784–3788.